Journal of the Korean Nuclear Society
Volume 27, Number 5, October 1995

Quantification of Realistic Discharge Coefficients for the Critical Flow Model of RELAP5/MOD3/KAERI

T.S. Kwon, B.D. Chung, W.J. Lee, N.H. Lee, and J.Y. Huh
Korea Atomic Energy Research Institute
(Received February 9, 1995)

RELAP5 / MOD3 / KAERI의 임계유동모델을 위한 실제적 배출계수의 정량화

권태순 · 정법동 · 이원재 · 이남호 · 허재영
한국원자력연구소
(1995. 2. 9 접수)

Abstract

The realistic discharge coefficients for the critical flow model of RELAP5/MOD3/KAERI are determined for the subcooled and two-phase critical flow by assessments of nine MARVIKEN Critical Flow Test(CFT). The selected test runs include a high initial subcooling and large nozzle aspect ratio(L/D). The code assessment results show that RELAP5/MOD3/KAERI over-predicts the subcooled critical flow and under-predicts the two-phase critical flow. Using these results, the realistic discharge coefficients of critical flow models are quantified by an iterative method. The realistic discharge coefficients are determined to be 0.89 for the subcooled critical flow and 1.07 for the two-phase critical flow, and the associated standard deviations are 0.0349 and 0.1189, respectively. The results obtained from this study can be applied to calculate the realistic system response of Large Break Loss of Coolant Accident and to evaluate the realistic Emergency Core Cooling System performance.

요 약

RELAP5/MOD3/KAERI의 임계유동모델을 위한 실제적인 배출계수들을 9개의 MARVIKEN 임계유동실험의 평가계산을 통하여 과냉각과 이상임계유동에 대하여 구하였다. 선택된 실험에는 높은 초기 과냉각도와 큰 노즐 세장비(L/D)인 것들이 포함되었다. 코드의 평가결과는 RELAP5/MOD3/KAERI은 과냉각임계유동을 크게 예측하고 이상임계유동은 작게 예측함을 보이고 있다. 이러한 결과들을 이용하여 임계유동모델의 실제적인 배출계수들을 반복법으로 정량화 하였다. 실제적인 배출계수는 과냉각임계유동이 0.89 그리고 이상임계유동이 1.07로 결정되었으며 관련 표준편차는 각각 0.0349과 0.1189이다. 본 연구로부터 얻어진 결과는 대형냉각재 상실사고의 실제적인 계통반응 계산과 비상노심냉각계통 성능평가에 적용할 수 있다.

1. Introduction

In a Loss of Coolant Accident (*LOCA*) analysis of Pressurized Light Water Reactor(*PLWR*), the accurate prediction of break flow through the break during blowdown phase is very important in evaluating the remaining coolant inventory. The coolant inventory has a first-order influence on the peak cladding temperature[1, 2]. During the blowdown phase of hypothetical Large Break Loss of Coolant Accident (*LBLOCA*), the system pressure and liquid inventory are strongly affected by the critical flow model. The high pressure safety injection(*HPSI*) flow rate, pressurizer pressure, containment back pressure, and total energy release rate through the break are also affected by the critical flow model. If the code over-predicts(under-predicts) the break flow rate it will increase(decrease) the energy release rate from RCS. The effect of critical flow model on the peak cladding temperature can be assessed through system integral effect tests. The calculated peak cladding temperature(*PCT*) in double ended guillotine break LOCA is strongly dependent on the discharge coefficient[3].

The rules on the ECCS evaluation method were revised by USNRC in 1988. The best-estimate(BE) analysis plus uncertainty concept was newly introduced in the revised rule(10CFR50.46). In the BE methodology, the model applicability and it's uncertainties should be quantified. Thus, the realistic discharge coefficient should be evaluated and shown to be capable of providing realistic discharge rates (Reg. Guide 1.157).

From 1960's, a number of separate and integral tests were performed to generate a critical flow database. These tests are well-categorized in reference 3. The separate tests are most useful to confirm the analytical model and empirical correlation of the critical flow. Integral tests are useful in confirming the integral modeling. But, some critical flow related data such as discharge conditions, flow conditions, and break mass flow rate are not well-reported in integral tests since the specific objectives of those tests are not for critical flow. Thus, the integral tests have some restrictions to use in the critical flow model confirmation. Before the MARVIKEN test, there existed only small-scale critical flow tests based over a wide range of test conditions and geometries. The MARVIKEN test is the first test that performed a critical flow measurement at a reactor scale, thus produced very useful data to confirm the critical flow models for the prototype reactors. From various studies for critical flow, it is known that the critical mass flux is governed by fluid states, stagnation enthalpy, nozzle inlet geometry, and nozzle aspect ratio (*L/D*)[4].

In this study, the realistic discharge coefficients for the critical flow model of RELAP5/MOD3/KAERI is quantified for the single phase and two-phase critical flow model respectively using nine-MARVIKEN tests. The results obtained from this study can be applied to calculate the realistic response of Large Break Loss of Coolant Accident and to evaluate the realistic Emergency Core Cooling System(*ECCS*) performance.

The quantification of realistic discharge coefficients for the critical flow model with respect to the LBLOCA blowdown thermal-hydraulics is performed as a part of the activities of the project "Development of LBLOCA KAERI-REM(Realistic Evaluation Model)" for developing the realistic code.

2. Review of the Critical flow Model and Test Description

2.1. Characteristics of the Critical Flow Model of RELAP5/MOD3/KAERI

In RELAP5/MOD3/KAERI, the choking flow is categorized into three cases with the criteria based on the break junction void fraction α_g. The three choking flows are defined as follows. [5]

$\alpha_g < 1.0\,E-05$: Subcooled choking flow (1)

$1.E-05 \le \alpha_g \le 0.1$: Transient choking flow (2)

$0.1<\alpha_g<0.9$: Two-phase choking flow (3)

In subcooled critical flow, the pressure undershoot method is applied to determine the local vaporization pressure for a sonic velocity at throat. A model described by Alamgir and Lienhard and Jones[*ALJ*] is used to calculate the local vaporization pressure at throat[5, 6]. In this model, the thermal non-equilibrium and slip(*non-homogeneous*) between two phases are considered. Non-equilibrium effects can result in vapor formation at a pressure considerably less than the local saturation pressure at the throat[5, 6]. The local vaporization pressure(P_t) is calculated as follows

$$P_{sat}-P_t = Max[0.0,\ (\delta P_{static}-\delta P_{turbulent})]$$

$$where,\ \delta P_{static}= -f\left(1+C_o\left(\frac{1}{A_t}\frac{dA_t}{dx}\right)^{0.8}V_c^{2.4}\right)^{1/2}$$

$$\delta P_{turbulent}=0.069984\left(\frac{A_t}{A}\right)^2 V_c^2 \quad (4)$$

t refers to throat, c refers to choked.

The static depressurization through the contraction of flow path, as given by Jones in eq.(4), is governed by nozzle contraction rate(dA/dx). Also, the local vaporization pressure(P_t) is affected by turbulent fluctuation. The turbulent fluctuation term ($\delta P_{turbulent}$) is varied with nozzle contraction ratio(A_t/A). Therefore, Non-equilibrium effects on the local vaporization pressure($P_{sat}-P_t$) are increased by nozzle contraction rate. However, the turbulent fluctuation effects on $P_{sat}-P_t$ are decreased with nozzle contraction ratio (A_t/A). Thus, the area change with spatial distance, dx, in the Jones pressure undershoot model is important, and is calculated differently. [5]

$$\left.\frac{dA}{dx}\right|_{Break} = \frac{A_{up}-A_j}{\Delta X_{up}/2}\ ,\ if\ smooth\ area\ change \quad (5)$$

$$\left.\frac{dA}{dx}\right|_{Break} = \frac{A_{up}-A_j}{10D_{up}}\ ,\ if\ abrupt\ area\ change \quad (6)$$

where, up refers to upstream volume and j refers to choked junction.

Therefore, the local vaporization pressure(P_t) is affected by nozzle length-to-diameter ratio(L/D). The smooth area change option should be applied to calculate the nozzle length effects on ALJ pressure undershoot model in eq.(4).

The ideal choking velocity is determined from the Bernoulli equation using pressure difference between the upstream pressure(P_{up}) and throat pressure(P_t). If the homogeneous equilibrium sound speed is larger than the result of the iterative solution from the pressure under-shoot method, the throat sonic velocity is reset to the saturated liquid homogeneous values.

The two-phase critical flow model is based on the analytic choking criteria described by Trapp and Ransom[5, 7] using a characteristic analysis of a two-fluid model. This model included relative phasic acceleration term since this term has a significant effect on the wave propagation. Also, Non-homogeneous and thermal equilibrium assumptions were employed. But, wall drag and heat transfers are not included into the characteristic analysis. Thus, nozzle length-to-diameter ratio is not effective in the two-phase critical flow model of RELAP5/MOD3/KAERI.

The user inputted discharge coefficient(C_d) is also factored into the sonic velocity. The final sonic velocity becomes

$$V_c = V_c\frac{ATHROT}{JCAT} * C_d \quad (7)$$

where, ATHROT refers to area ratio, JCAT refers to density ratio[5]

2.2. Test Matrix

MARVIKEN test is a simplified critical flow test with both subcooled and saturated liquid. The facility consists of three major components; a pressurized vessel, a discharge pipe, and a test nozzle. The test facility and test conditions are well described in reference 7. The fluid is discharged from a nearly full sized vessel with respect to reactor vessel of nuclear plant through a large diameter discharge pipe that

Table 1. Initial and Discharge Conditions at Vessel Bottom.

Test No.	Nozzle			Steam Dome Pressure & Temperature		Subcooling at Vessel Bottom	Vessel Water level	Test period
	D (mm)	L (mm)	L/D	(MPa)	(C)	(C)	(M)	(sec)
3	509	1589	3.1	5.02	264	22	17.06	42
4	509	1589	3.1	4.94	264	37	17.59	49
8	509	1589	3.1	4.95	263	35	17.51	49
11	509	1589	3.1	4.97	264	35	17.63	48
15	500	1809	3.6	5.04	264	31	19.93	55
16	500	1809	3.6	5.00	264	33	17.63	49
21	500	730	1.5	4.94	263	33	19.95	60
22	500	730	1.5	4.93	263	52	19.64	48
27	500	730	1.5	4.91	263	33	19.82	59

supplied the flow to the test nozzle. The pressurized vessel has an inside diameter of 5.22m and a height of 24.55m from the vessel bottom to the top-cupola. The discharge pipe has dimensions of 0.752m in diameter and 6.3m in length. The nozzle length-to-diameter(L/D) ratio ranges from 0.33 to 3.7 The test nozzle has a well-rounded inlet, having a radius of curvature equal to the nozzle radius. The mass flux for well-rounded entrance geometries are higher than the corresponding sharp entrance [4].

To assess the critical flow model of RELAP5/MOD-3/KAERI, nine Critical Flow Tests(*CFT*) are simulated. Selected tests are characterized by high initial subcooling degree, high length-to-diameter ratio($L/D\rangle 1.5$), and the nozzle diameter larger than 0.5 meter. The initial and discharge conditions of CFTs are summarized in Table 1. The phase transition time is affected by the initial subcooling degree at the vessel bottom. Therefore, to assess the subcooled critical flow model for the long period, the data group of high subcooling degree was selected. In addition, to minimize the scale effects, the data group of large nozzle diameter was selected. In MARVIKEN tests, the effect of nozzle length-to-diameter ratio on the critical mass flux under subcooled stagnation conditions diminishes for nozzle length-to-diameter ratios larger than approximately 1.5. Further increase in length does not reduce the mass flux appreciably. Also, the effect of nozzle length on the critical mass flux under saturated stagnation conditions shows that the mass fluxes decrease with increasing length, but the variations are within the specified experimental error limits[8]. Therefore, the data group of L/D$\rangle$1.5 was selected to minimize the effect of nozzle length-to-diameter ratio.

3. Analysis Methods and Models

3.1. Nodalization of Test Facility

For the separate effect test of critical flow model, the simplified evaluation model is adopted to minimize the effects of other analytic model in the code. A simplified nodalization and boundary conditions were adopted for this assessment. The nodalization diagram is shown in Fig. 1. A time dependent volume(*TMDPVOL*) component was used to represent the pressure vessel, and the discharge inlet conditions at vessel bottom are determined from the experimental data. This model gives the minimum disturbance of water properties in the downstream node of the vessel. The containment was also represented

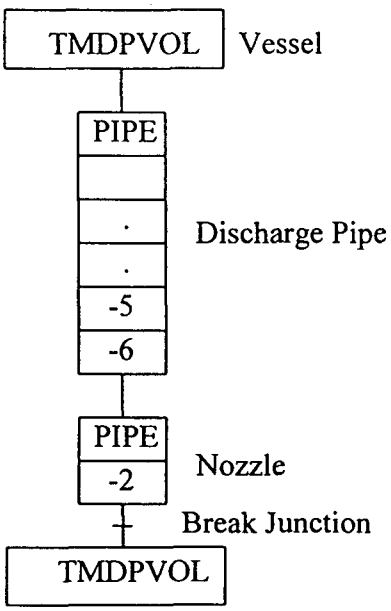

Fig. 1. Nodalization Diagram

by a TMDPVOL component. The discharge pipe between the vessel and the nozzle was represented by a PIPE component with 6-cell. The nozzle was represented by a PIPE component with 2-cell.

3.2. Boundary Conditions

For the subcooled critical flow, the measured pressure and temperature at the vessel bottom were used as the conditions of TMDPVOL. After the fluid condition at the vessel bottom reached near saturation, the boundary conditions were replaced with saturated conditions for the two-phase critical flow. The pressure and fluid quality at the vessel bottom were fed as the discharge pipe inlet conditions. Although the fluid condition at the vessel bottom did not reach saturation, the pattern of the subcooling reached a plateau without decreasing or increasing, and this condition was treated as a saturation condition. To minimize the disturbance of choking location near the break node, the choking option was applied only at the nozzle outlet(*break*) junction. Allowing only one choking option at the nozzle without the unphysical oscillation. The smooth area change option was applied to the nozzle outlet junction.

3.3. Quantification Procedure of Realistic Discharge Coefficients

To determine the best estimated discharge coefficients, trial-and-error method was applied separately for subcooled and two-phase choking flow regime since the variation rate of discharge coefficient vs. discharge mass flow rate was not constant(*non-linear*). In RELAP5/MOD3/KAERI, there are three user inputted discharge coefficients for subcooled, two-phase, and super-heated vapor. However, in this study, only the subcooled and the two-phase discharge coefficients are considered since these coefficients have the most dominant effect on the break mass flow in LOCA analysis.

For realistic discharge coefficients, the subcooled and two-phase choked flow are re-categorized with junction void fraction α_g as eq.(8) and eq.(9) instead of eq.(1) and eq.(3).

$$\alpha_g < 1.0\,E-05 : \text{Subcooled choking flow} \quad (8)$$

$$\alpha_g > 0.3 : \text{Two-phase choking flow} \quad (9)$$

To quantify the best-fitness of discharge coefficient, a predictability determined by statistical method, was introduced for each flow regime. The predictability of discharge coefficient is defined as follow.

$$P_i = \frac{1}{N_i}\sum_{j=1}^{N_i}\frac{MM_i(j)}{MC_i(j)} \quad (10)$$

where, i = *subcooled, two-phase*

MM = *measured mass flow rate*

MC = *calculated mass flow rate*

N_i = *number of data for each flow regime*

$= N_{CFT3} + N_{CFT4} + N_{CFT8} \cdots + N_{CFT22} + N_{CFT27}$

The predictability of 1 in eq.(10) means that the bias between the calculated and the measured mass is zero. To obtain the predictability, the realistic subcooled discharge coefficient was determined first and

then the two-phase discharge coefficient was quantified. The convergence criteria of predictability for iterative runs was set to 0.99. If the predictability is less than 0.99(*99% well-fitted*), the discharge coefficient C_d^{iter+1} is replaced with new value obtained by multiplying the predictability and the discharge coefficient at the previous run in the given flow regime. The new discharge coefficient is replaced as follow.

$$C_{d,i}^{iter+1} = C_{d,i}^{iter} * P_i^{iter} \quad (11)$$

where, iter = iteration in each flow regime

The quantification procedures are as follow. 1) Set discharge coefficient for subcooled choked flow. 2) Quantify the predictability of discharge coefficient using calculated and experimental mass flow rate data using eq.(10). 3) Reset discharge coefficient with new value obtained by multiplying the predictability and the discharge coefficient at the previous step. 4) Repeat step 2 and step 3 until the predictability becomes nearly one. 5) Repeat step 1 to step 4 for two-phase choked flow. The total number of data used was 1021 for the subcooled choked flow, and 1585 for the two-phase choked flow. The transition discharge coefficient was not quantified because the transition critical flow rate is calculated by linear interpolation between the subcooled and two-phase critical flow.

4. Nozzle Noding and Area Change Option Effects

The subcooled critical mass flux is mainly affected by area difference between upstream and break junction, area change option, and nozzle length-to-diameter ratio(L/D). As shown in eq.(4), the local vaporization pressure in RELAP5/MOD3/KAERI critical flow model for subcooled critical flow is strongly governed by the flow area contraction rate(dA/dx). MARVIKEN tests have a straight-pipe type nozzle which does not have a throat. Therefore, if the straight nozzle is considered in the nodalization as shown in Fig. 2(b), the spatial derivative of area at break(dA/dx) becomes zero because the upstream flow area(A_{up}) is equal to break(*throat*) junction area(A_{break}). Thus, the area change option does not affect the critical mass flux in this condition.

The nozzle modeling sensitivity study was performed using flow system given in Fig. 2(a); ($A_{up} > A_{break}$) and Fig. 2(b); ($A_{up} = A_{break}$). A very short nozzle was represented by the (a) type flow geometry of Fig. 2, also a straight nozzle was represented by the (b) type flow geometry of Fig. 2. The nozzle was modeled as SINGLE JUNCTION component for the (a) type flow model of Fig. 2, also was modeled as PIPE component for the (b) type flow model of Fig. 2. The main difference between the above two flow models is the flow area of upstream node. The flow area of upstream node contribute to the spatial derivative of

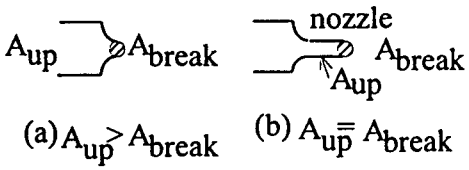

Fig. 2. Break Upstream Area with Nozzle Modeling (a) dA/dx> 0 (b) dA/dx=0

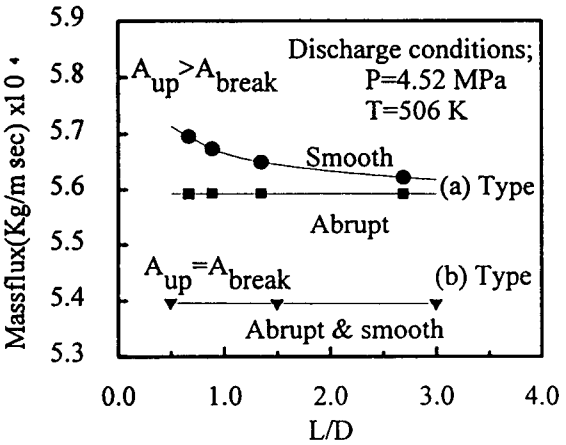

Fig. 3. Mass Flux vs. Nozzle L/D and Junction Area Change Option for the Flow Types of Fig.2

flow area at break junction as mentioned in eq.(5) and eq.(6). The results of sensitivity studies are shown in Fig. 3. The mass flux for the SINGLE JUNCTION(*(a) type flow model of Fig. 2)* model of nozzle is larger than that of PIPE model. If the nozzle modeled with SINGLE JUNCTION component for the (a) type flow model of Fig. 2, the discharge pipe contributes to the spatial derivative of area instead of nozzle. The mass flux using abrupt area change option is nearly constant for both SINGLE JUNCTION and PIPE model of the nozzle since the spatial derivative of area is considered to be constant by eq. (6). However, if the smooth area change option was applied in the above two flow models, the mass flux has different behaviors with L/D. The mass flux for the SINGLE JUNCTION model of nozzle which is (a) type flow model of Fig. 2 decreases with L/D. But the corresponding mass flux for the PIPE model of nozzle does not change with L/D since the spatial derivative of flow area is zero($A_{up} = A_{break}$). The critical mass flux of the (b) type flow model of Fig. 2 is independent of node length-to-diameter in the nodalization. These results mean that the critical mass flux of SINGLE JUNCTION model for the (b) type flow geometry of Fig. 2 under the same discharge conditions and discharge coefficients is larger than that of PIPE model.

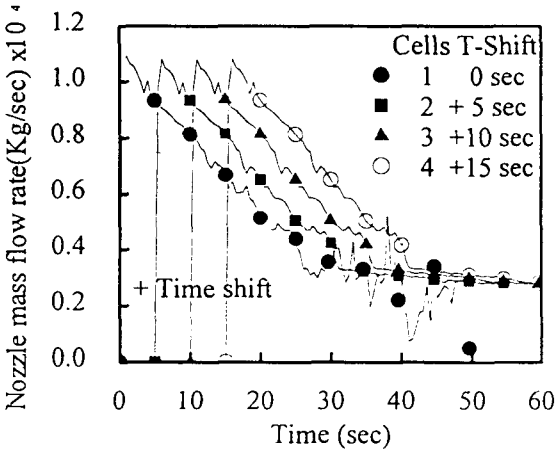

Fig. 4. Nozzle Noding Sensitivity Study with CFT21

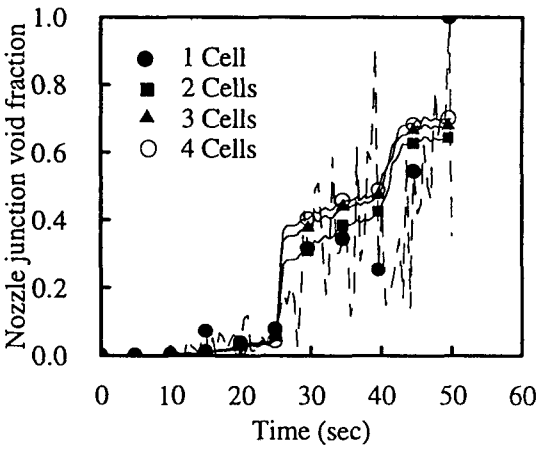

Fig. 5. Nozzle Noding Sensitivity Study with CFT21

For the simulation of nozzle noding sensitivity stud y, the nozzle was modeled by PIPE component with number of cells ranging from 1 to 6. The discharge area was represented by a SINGLE JUNCTION component. As shown in Fig. 4, the subcooled critical mass flowrates are little affected by the number of cells of the nozzle. The sudden flow area contraction effects on mass flux of the straight-pipe type nozzle ($A_{break} = A_{nozzle}$) are not considered properly on the local vaporization pressure of ALJ model since the area change rate always becomes zero. The two-phas e critical flowrates are nearly the same for all cases except the single-cell case. These trends are also seen in Fig. 5. The void fractions in the two-phase critical flow increased with number of nozzle cells. Also, the high spikes of void fraction appeared in the single-cell case, hence 2-cell model(node length-to-diameter ratio, $L/D=0.75\sim1.55$) was adopted for the nozzle(L/D>1.5). The calculated critical mass flowrates of straight nozzle in the model are not sensitive on the volume length-to-diameter ratio and area change options since the area change(dA) becomes zero.

5. Best-estimate Discharge Coefficients

For realistic discharge coefficients, the nozzle was

modeled by a PIPE component. The area change option for the nozzle of straight pipe type, in RELAP5/MOD3/KAERI critical flow model, is not considered since the upstream area of break junction is equal to the break junction area. As discussed in Fig. 2, the abrupt and smooth area change option at break junction of straight type nozzle($A_{break} > A_{nozzle}$) is not effective for the critical mass flux. The predictability of critical flow model was confirmed separately. The results are shown in Fig. 6 for the subcooled choking flow, shown in Fig. 7 for the two-phase choking flow, and shown in Fig. 8 for the integrated discharged mass for the subcooled and two-phase critical flow. The calculated critical mass flowrates are in fairly good agreement with the experimental data when the value of 0.89 for the subcooled choking flow and the value of 1.07 for the two-phase choking flow are applied. The integrated discharged mass through the nozzle, as shown in Fig. 8, is compared to confirm the quantified realistic discharge coefficients. The calculated discharged mass is in fairly good agreement with experimental data. The realistic discharge coefficients and associated standard deviations are summarized in Table 2.

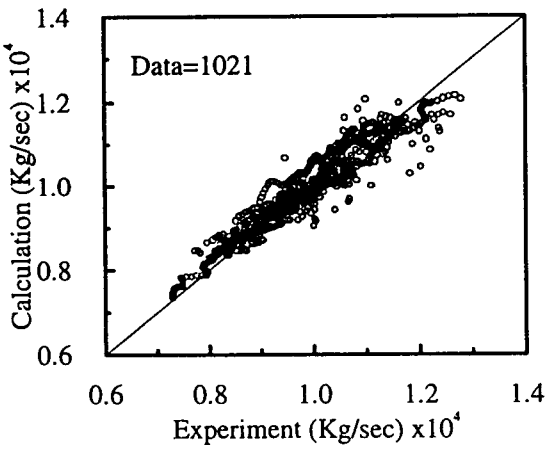

Fig. 6. Comparison of Experimental vs. Calculational Mass Flow rate for Subcooled Critical Flow

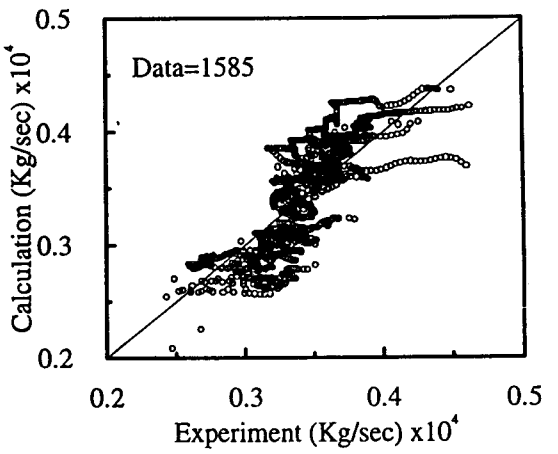

Fig. 7. Comparison of Experimental vs. Calculational Mass Flow rate for Two-Phase Critical Flow

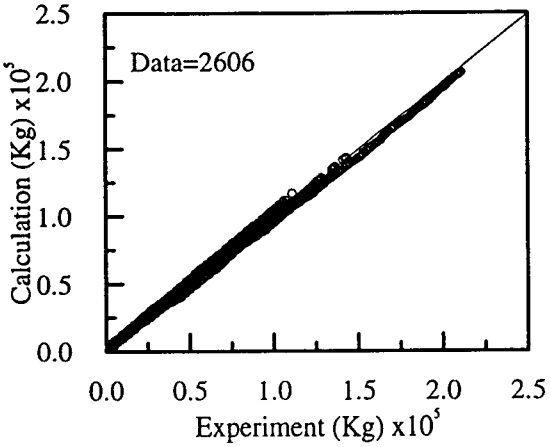

Fig. 8. Comparison of Experimental vs. Calculational Integrated Discharge Mass for Subcooled and Two-Phase Critical Flow

Table 2. Discharge Coefficients and Standard Deviations

	Discharge Coefficient	Standard Deviation
Subcooled	0.89	0.0349
Two-phase	1.07	0.1189

6. Conclusions

The realistic discharge coefficients for the critical flow model of RELAP5/MOD3/KAERI are quantified by a statistical method using MARVIKEN 9 CFTs data. The best fitted discharge coefficients and the standard deviations for the subcooled and the two-phase critical flow are determined. After assessment, following results are obtained.

(1) The subcooled critical flow model of RELAP5/MOD3/KAERI over-predicts the critical mass flow rate. When the nozzle is included in the system modeling, the best-estimate discharge coefficient for subcooled critical flow is 0.89, and the associated standard deviation is 0.0349.

(2) The two-phase critical flow model of RELAP5/MOD3/KAERI generally under predicts the critical mass flow rate. When the nozzle is included in the system modeling, the best-estimate discharge coefficient for the two-phase critical flow is 1.07, and associated standard deviation is 0.1189.

(3) The number of cells of the upstream volume has little effect on the calculated critical mass flow rates. When the nozzle is modeled by a pipe component, the break junction area is equal to the upstream volume area. Thus, the area change options both abrupt and smooth are not effective on the break discharge mass.

(4) In the nodalization, the effect of volume length-to-diameter ratio(L/D) on the critical mass flux is negligibly small for the straight type nozzle.

References

1. Upendra S. Rohatgi et al., "Uncertainty in Modeling and Scaling of Critical Flow in TRAC-PF1/MOD1", NUREG/CR-5249, December (1989)
2. "Compendium of ECCS Research of Realistic LOCA Analysis", NUREG-1230, April (1987)
3. B.D. Chung et al., "Quantification of Reactor Safety Margins for Large Break LOCA with Application of Realistic Evaluation Methodology", Journal of the Korean Nuclear Society, Volume 26, Number 3, Sep (1994)
4. D. Abdollahian et al., "Critical Flow Data Review and Analysis", EPRI-NP-2192, January (1982)
5. K.E. Carlson et al., "RELAP5/MOD3 Code Manual Volume IV: Models and Correlations", NUREG/CR-5535, June (1990)
6. V.H. Ransom and J.A. Trapp, "The RELAP5 Choked Flow Model and Application to a Large Scale Flow Test", Proceeding of the ANS/ASME/NRC International Topical Meeting on Nuclear Reactor Thermal-Hydraulics, Saratoga Springs, NewYork, Oct. 5－8, pp 799－819 (1980)
7. J.A. Trapp and V.H. Ransom, "A Choked-Flow Calculation Criterion for Non-homogeneous, Non-equilibrium, Two-Phase Flows", International Journal of Multiphase Flow, 8, pp 669－681 (1982)
8. Studsvik Energieknik AB, "The MARVIKEN Full-Scale Critical-Flow Tests", EPRI-NP-2370, December, Final report Vol 1－35 (1982)